SUPPORTING INFORMATION

Agonists for 13 Trace Amine-Associated Receptors provide insight into the molecular basis of odor selectivity

David M. Ferrero[1], Daniel Wacker[2], Miguel Roque[1], Maude W. Baldwin[3], Raymond C. Stevens[2], and Stephen D. Liberles[1,*]

[1]Department of Cell Biology, Harvard Medical School, Boston, MA 02115, USA.

[2]Department of Molecular Biology, The Scripps Research Institute, La Jolla, CA 92037, USA.

[3]Department of Organismic and Evolutionary Biology, Harvard University, Cambridge, MA 02138, USA.

*Corresponding Author: e-mail: Stephen_Liberles@hms.harvard.edu,

phone: (617) 432-7283, fax: (617)-432-7285

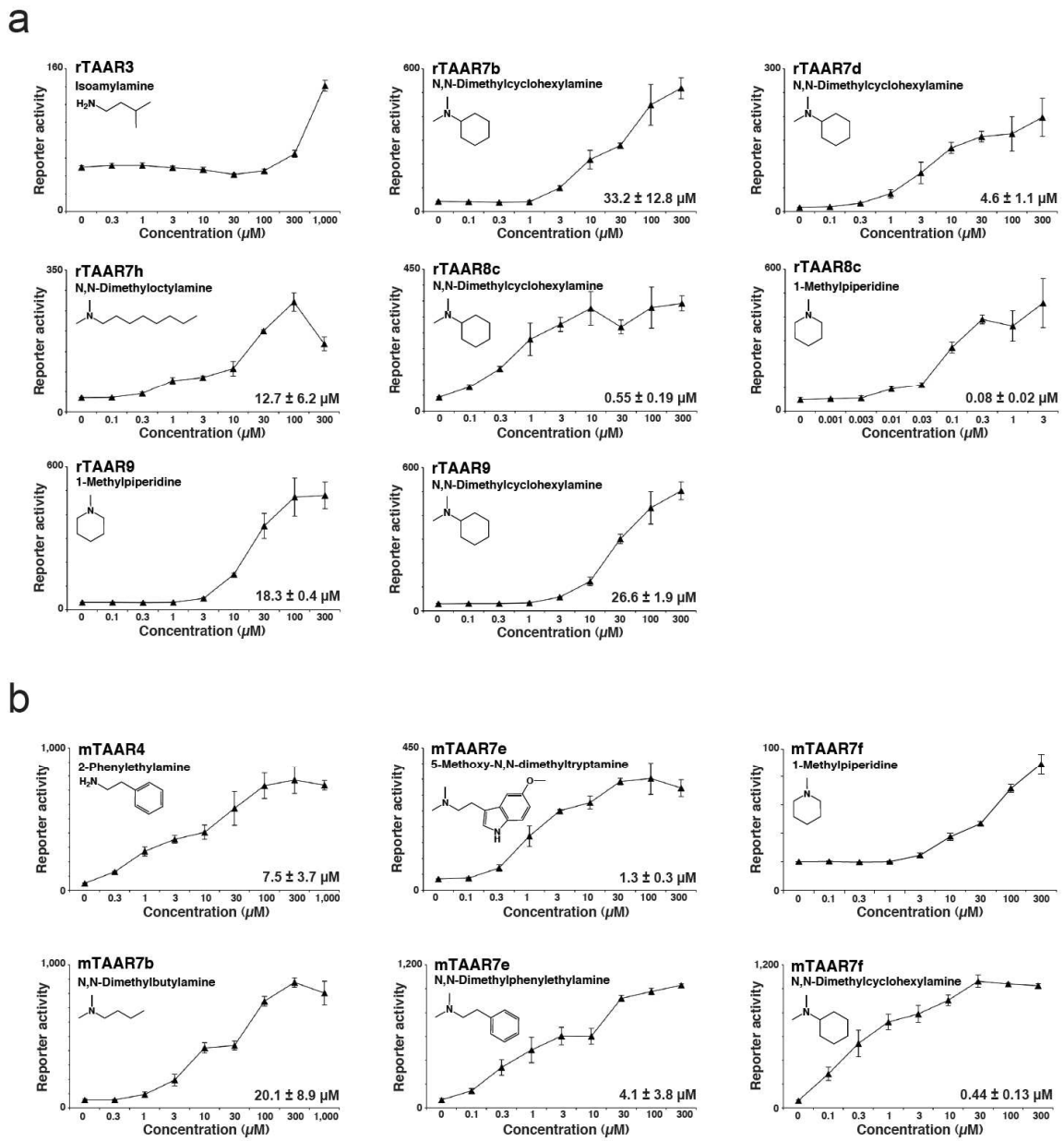

Supplementary Figure 1 Dose-dependent responses of TAARs to amines. HEK293 cells were cotransfected with plasmids encoding CRE-SEAP and rTAARs (a) or mTAARs (b), incubated with concentrations of ligands indicated, and assayed for reporter activity (triplicates ± s.d.). EC_{50} values (± s.e.m, bottom right) were calculated using SigmaPlot (Systat Software) and a 4-parameter Hill equation. EC_{50} values for receptor-ligand interactions that did not reach saturation are not determined.

Percentage identity between TAAR orthologs (amino acid)

	mouse vs. rat	mouse vs. human	rat vs. human
TAAR1	86	75	78
TAAR2	97	89	89
TAAR3	96	-	-
TAAR4	94	-	-
TAAR5	96	86	84
TAAR6	94	88	87
TAAR7	84-94	-	-
TAAR8	90-93	78-80	78-80
TAAR9	95	86	86

Supplementary Figure 2 Percentage amino acid identity between TAAR orthologs of mouse, rat, and human, calculated using ClustalW.

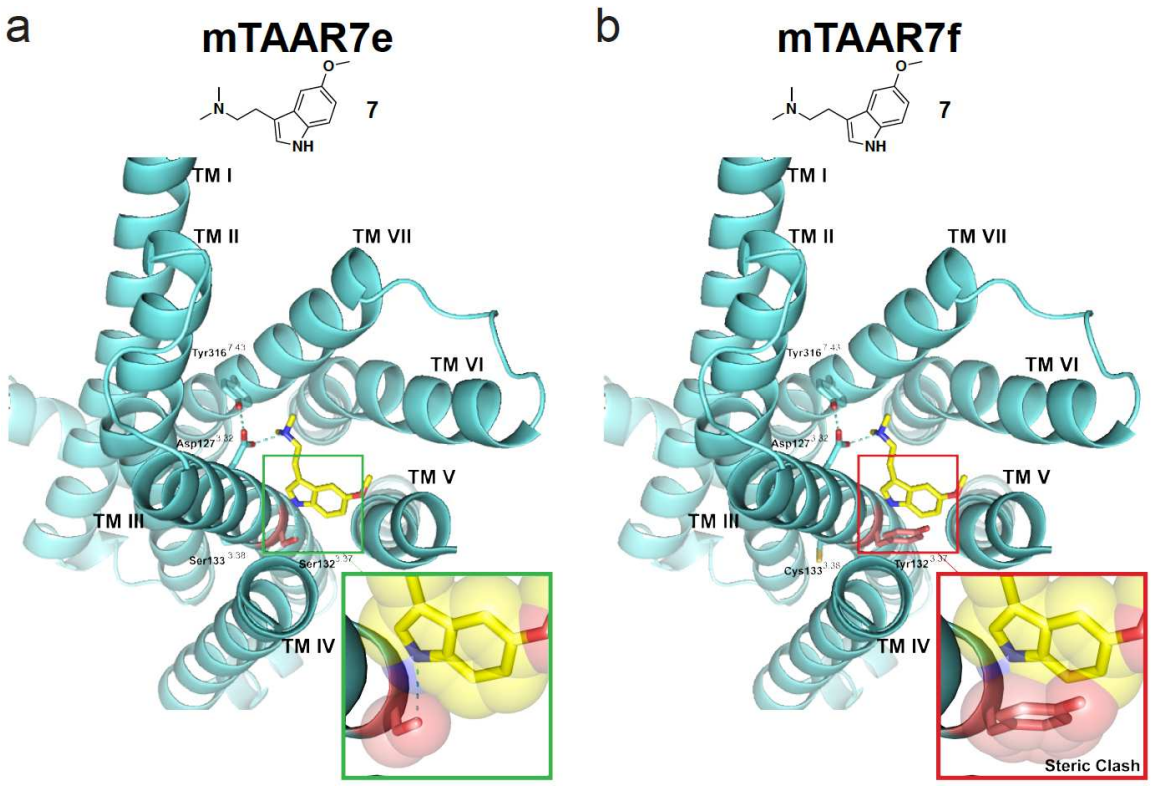

Supplementary Figure 3 Homology modeling of mTAAR7e and mTAAR7f bound to 5-methoxy-N,N-dimethyltryptamine (**7**). Predicted structures (cyan) of mTAAR7e (a) and mTAAR7f (b) bound to **7** (yellow). GPCR transmembrane helices are numbered TM I to VII and side chains of key residues that line the ligand binding site are displayed. Hydrogen bonds are shown as dotted cyan lines. Inserts represent a magnified view of **7** interacting with residue $132^{3.37}$ of mTAAR7e and mTAAR7f. Van der Waals radii are shown with a space-filling model, and predict a steric clash of **7** with residue $Tyr132^{3.37}$ of mTAAR7f but not $Ser132^{3.37}$ of mTAAR7e.

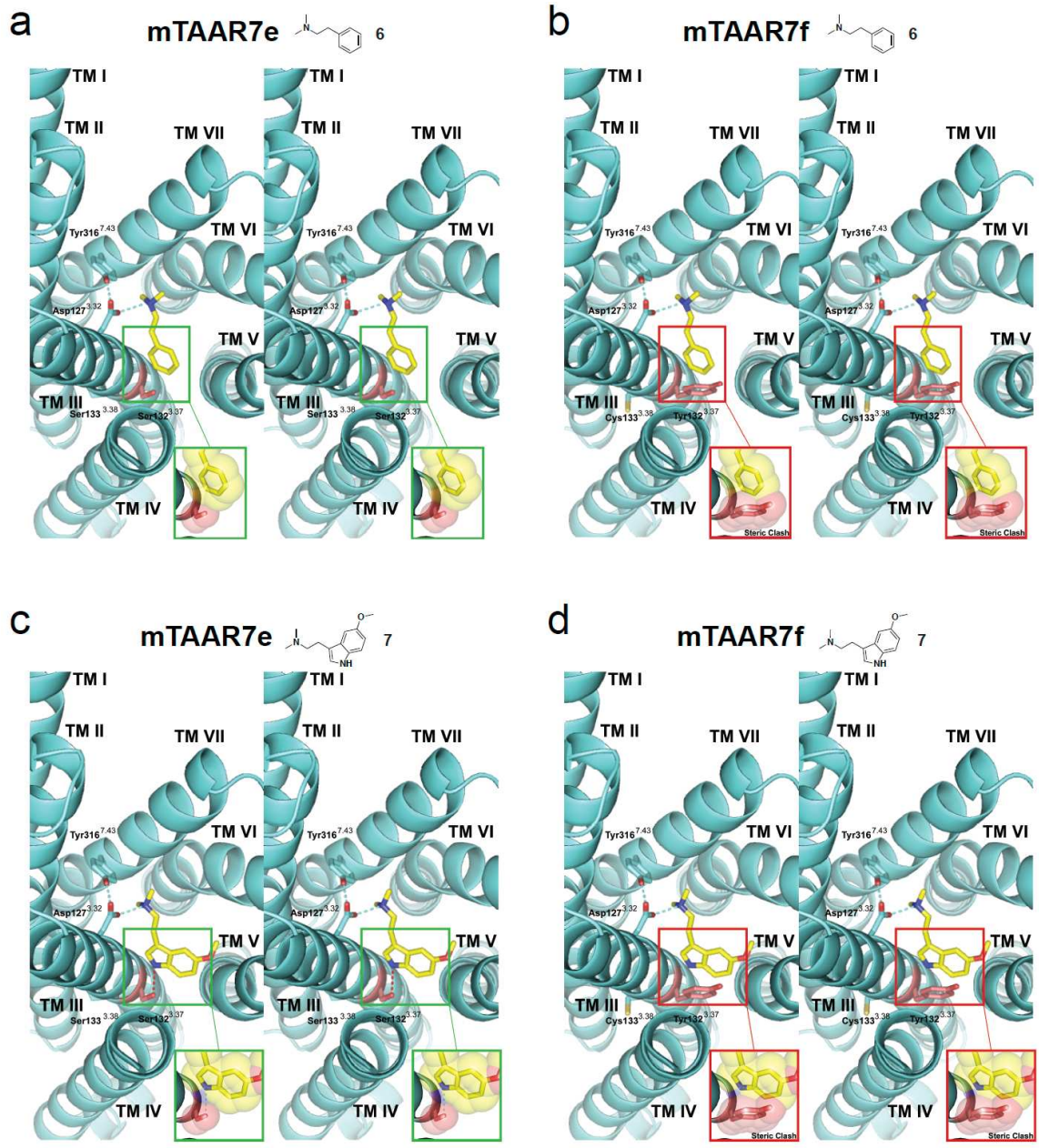

Supplementary Figure 4 Homology models of mTAAR7e and mTAAR7f bound to N,N-dimethylphenylethylamine (**6**) and 5-methoxy-N,N-dimethyltryptamine (**7**), shown in stereo.

SUPPLEMENTARY METHODS

Chemicals tested for mTAAR agonism. Chemicals tested for the ability to activate mouse TAARs include those previously described (*1*), as well as the following mixes (5 μM of each indicated compounds). **Mix 1**: N,N-dimethyl-cyclohexylamine, N,N-dimethyl-phenylethylamine, creatinine, taurine. **Mix 2**: N-methyl-pyrrolidine, N,N-dimethyl-octylamine, N,N-dimethyl-butylamine, N,N-dimethyl-isopropylamine. **Mix 3**: N-methyl-proline, N-methyl-glycine, 4-(dimethylamino)-butyric acid, 3-(dimethylamino)-benzoic acid. **Mix 4**: 2-dimethylamino-2-methyl-1-propanol, 3-dimethylamino-1-propanol, 1-dimethylamino-2-propanol. **Mix 5**: N,N-dimethyl-p-phenylenediamine, N,N-dimethyl-ethylenediamine, tetramethyl-1,4-butanediamine, 2-(dimethylamino)-ethanethiol. **Mix 6**: pyridine N-oxide, N,N-dimethyl-benzylamine, N,N-dimethyl-aniline, N,N-dimethyl-1-naphtylamine. **Mix 7**: 6-(dimethylamino)-purine, 2-dimethylamino-6-hydroxypurine, 5-methoxy-N,N-dimethyltryptamine, 1-methylindole, gramine. **Mix 8**: dansyl cadaverine, dimethylurea, (dimethylamino)-acetaldehyde-diethylacetal, N,N-dimethyl-acetamide, 3-(dimethylamino)-propiophenone.

Chemicals tested for rTAAR agonism. The following mixes (10 μM of each indicated compounds) were tested for their ability to activate rat TAARs. **Mix 1**: butylamine, dibutylamine, hexylamine. **Mix 2**: 2-aminopentane, isoamylamine, isobutylamine, isopropylamine. **Mix 3**: N,N-dimethylcyclohexylamine, 1-methylindole, tryptamine, phenylethylamine. **Mix 4**: indole, 1-methylpyrrolidine, 1-methylpiperidine, pyrrolidine. **Mix 5**: ethylenediamine, cadaverine dihydrochloride, 1,4-diaminobutane dihydrochloride. **Mix 6**: benzylamine, 1-methylhistamine dihydrochloride, histamine dihydrochloride. **Mix 7**: GABA, ß-alanine, cystamine dihydrochloride, histamine dihydrochloride. **Mix 8**:

methylamine, dimethylamine, trimethylamine. **Mix 9**: tyramine hydrochloride, octopamine hydrochloride, 3-methoxytyramine, 3,4-dimethoxyphenethylamine, 4-methoxyphenethylamine, N,N-dimethylphenethylamine. **Mix 10**: 5-hydroxyindole-3-acetic acid, 5-aminoindole hydrochloride, 5-methoxytryptamine, 5-methoxy-N,N-dimethyltryptamine, gramine. **Mix 11**: aniline hydrochloride, A-naphtylamine. **Mix 12**: 2,5-dimethylpyrazine, 3-(dimethylamino)-propiophenone. **Mix 13**: agmatine sulfate, tetramethylammonium chloride, creatinine hydrochloride, 1-(2-aminoethyl)-pyrrolidine, tetramethyl-1,4-butanediamine. **Mix 14**: 2-methylbutylamine, 3-(methylthio)-propylamine, cyclohexylamine, N,N-dimethylbenzoic acid, N,N-dimethylisopropylamine. **Mix 15**: cysteamine hydrochloride, amino-2-propanol, N,N-dimethylethanol amine, 1-dimethylamine-2-propanol, 2-(dimethylamino)-ethanethiol. **Mix 16**: 4-aminobenzoic acid, N,N-dimethylglycine hydrochloride, taurine.

TAAR functional assays. Full *Taar* coding regions were cloned into pcDNA3.1- (Invitrogen) with or without a 5' DNA extension of 69 bp encoding the first 20 amino acids of bovine rhodopsin followed by a cloning linker (GCGGCCGCC). Point mutations were introduced in mTAAR7e and mTAAR7f by overlap extension PCR. Functional assays were performed as described (*1, 2*). Fluorescence was measured on an EnVision plate reader (Perkin Elmer) and SEAP activity graphed as relative fluorescence of a phosphatase substrate.

Phylogenetic analysis. Full-length *Taar* coding sequences were aligned with the multiple sequence alignment program MAFFT (Multiple Alignment using Fast Fourier Transform) (*3*), using a mouse olfactory receptor (MOR-1362) and five mouse biogenic amine receptors (histamine H2 receptor, serotonin 1a and 5a receptors, dopamine 2 and 3

receptors) as outgroups. The best-fitting nucleotide substitution model, GTR+I+Γ, was selected using Akaike Information Criterion (AIC) implemented in the program MRMODELTEST (*5*). The phylogenetic tree was constructed using the program MRBAYES 3.1.2 (*6*) using default priors, except for the branch length prior for which an exponential distribution with unconstrained values was used. MRBAYES was run for 10,000,000 generations with 4 Markov chains, and sampling occurred every 1,000 generations. The trees from the first 1,000,000 generations were discarded as burn-in. Nodal support values were estimated by Bayesian posterior probabilities.

Generation of mTAAR homology models. 3D models of mTAAR7e and mTAAR7f were generated with the molecular modeling package ICM (Version 3.6.-1b, Molsoft LLC) that uses the ZEGA alignment algorithm (*7*) and the standard modeling function BuildModel (*8*). Both models were based on the structure of the nanobody stabilized β_2 adrenergic receptor (β_2AR) bound to the agonist BI-167107 (PDB ID: 3P0G) (*9*), using only the receptor coordinates. The alignment between the TAARs and the structured regions of β_2AR shows 33% sequence similarity and it was manually adjusted to eliminate minor gaps in TM helix I and the C-terminus. Intracellular loop 3 (ICL3) of both mTAARs was not aligned since the β_2AR construct contains a T4 Lysozyme molecule that replaces ICL3 but is disordered in the structure. A limited energy-based optimization of side chains and loops was done after the coordinates were placed according to the alignment and the 3P0G coordinates. The ligands were placed into the models using COOT (*10*) and the data was evaluated and figures were made in PyMOL.

SUPPLEMENTARY REFERENCES

1. Liberles, S. D., and Buck, L. B. (2006) A second class of chemosensory receptors in the olfactory epithelium, *Nature 442*, 645-650.
2. Ferrero, D. M., Lemon, J. K., Fluegge, D., Pashkovski, S. L., Korzan, W. J., Datta, S. R., Spehr, M., Fendt, M., and Liberles, S. D. Detection and avoidance of a carnivore odor by prey, *Proc Natl Acad Sci U S A 108*, 11235-11240.
3. Katoh, K., Misawa, K., Kuma, K., and Miyata, T. (2002) MAFFT: a novel method for rapid multiple sequence alignment based on fast Fourier transform, *Nucleic Acids Res. 30*, 3059-3066.
4. Thompson, J. D., Higgins, D. G., and Gibson, T. J. (1994) CLUSTAL W: improving the sensitivity of progressive multiple sequence alignment through sequence weighting, position-specific gap penalties and weight matrix choice, *Nucleic Acids Res 22*, 4673-4680.
5. Posada, D., and Crandall, K. A. (1998) MODELTEST: testing the model of DNA substitution, *Bioinformatics 14*, 817-818.
6. Ronquist, F., and Huelsenbeck, J. P. (2003) MrBayes 3: Bayesian phylogenetic inference under mixed models, *Bioinformatics 19*, 1572-1574.
7. Abagyan, R. A., and Batalov, S. (1997) Do aligned sequences share the same fold?, *J Mol Biol 273*, 355-368.
8. Cardozo, T., Totrov, M., and Abagyan, R. (1995) Homology modeling by the ICM method, *Proteins 23*, 403-414.
9. Rasmussen, S. G., Choi, H. J., Fung, J. J., Pardon, E., Casarosa, P., Chae, P. S., Devree, B. T., Rosenbaum, D. M., Thian, F. S., Kobilka, T. S., Schnapp, A., Konetzki, I., Sunahara, R. K., Gellman, S. H., Pautsch, A., Steyaert, J., Weis, W. I., and Kobilka, B. K. Structure of a nanobody-stabilized active state of the beta(2) adrenoceptor, *Nature 469*, 175-180.
10. Emsley, P., Lohkamp, B., Scott, W. G., and Cowtan, K. Features and development of Coot, *Acta Crystallogr D Biol Crystallogr 66*, 486-501.